J. Appl. Cryst. (1996). **29**, 134–146

Small-Angle Scattering from Polymeric Mass Fractals of Arbitrary Mass-Fractal Dimension

G. BEAUCAGE

Department of Materials Science and Engineering, University of Cincinnati, Cincinnati, OH 45221-0012, USA

(*Received* 2 *May* 1995; *accepted* 21 *August 1995*)

Abstract

The Debye equation for polymer coils describes scattering from a polymer chain that displays Gaussian statistics. Such a chain is a mass fractal of dimension 2 as evidenced by a power-law decay of -2 in the scattering at intermediate q. At low q, near $q \simeq 2\pi/R_g$, the Debye equation describes an exponential decay. For polymer chains that are swollen or slightly collapsed, such as is due to good and poor solvent conditions, deviations from a mass-fractal dimension of 2 are expected. A simple description of scattering from such systems is not possible using the approach of Debye. Integral descriptions have been derived. In this paper, asymptotic expansions of these integral forms are used to describe scattering in the power-law regime. These approximations are used to constrain a unified equation for small-angle scattering. A function suitable for data fitting is obtained that describes polymeric mass fractals of arbitrary mass-fractal dimension. Moreover, this approach is extended to describe structural limits to mass-fractal scaling at the persistence length. The unified equation can be substituted for the Debye equation in the RPA (random phase approximation) description of polymer blends when the mass-fractal dimension of a polymer coil deviates from 2. It is also used to gain new insight into materials not conventionally thought of as polymers, such as nanoporous silica aerogels.

1. Introduction

The application of mass scaling laws to scattering from disordered materials has led to an understanding of weak power-law decays in terms of mass-fractal morphologies (Schmidt, 1992; Korberstein, Morra & Stein, 1980; Debye, Henderson & Brumberger, 1957; Fisher & Burford, 1967). These power-law decays display power-law slopes shallower than -3. Several authors have noted that mass-fractal scaling regimes display limits at high and low q related to size limits to mass-fractal scaling (Lin, Klein, Lindsay, Weitz, Ball & Meakin, 1990; Schaefer & Hurd, 1990; Wiltzius, Bates, Dierker & Wignall, 1987; Mountain & Mulholland, 1988; Mountain, Mulholland & Baum, 1986; Hurd, 1990). Recently, a description for these limits to mass-fractal scaling and their associated scattering power-laws has been presented (Beaucage, 1995; Beaucage & Schaefer, 1994; Beaucage, Ulibarri, Black & Schaefer, 1995; Ulibarri, Beaucage, Schaefer, Olivier & Assink, 1992; Hua, Anderson, Hareid, Smith & Beaucage, 1994; Schaefer, Pekala & Beaucage, 1995). Although an approximate form, this unified approach has been demonstrated to duplicate closely exact calculations for mass fractals, surface fractals, diffuse-interfaced particulate systems and structural systems displaying multiple structural levels such as rods and lamellae (Beaucage, 1995). It has also been used extensively to fit experimental data (Beaucage & Schaefer, 1994; Beaucage, Ulibarri, Black & Schaefer, 1995; Ulibarri, Beaucage, Schaefer, Olivier & Assink, 1992; Hua, Anderson, Hareid, Smith & Beaucage, 1994; Schaefer, Pekala & Beaucage, 1995).

The unified equation describes a material over a wide range of sizes in terms of structural levels. One structural level pertains to a Guinier regime, describing an average structural size, and a power-law regime, describing the mass- or surface-fractal scaling for that structural level. Any number of structural levels can be described in this parameterization of morphology.

In this paper, the unified approach is applied to mass-fractal structures. Specifically, fractal ideas native to disordered materials will be applied to polymeric morphologies. A description of scattering from polymer coils that allows for arbitrary mass scaling results from this comparison. The hybrid equations can in turn be used to describe mass-fractal morphologies throughout the disordered materials field. Insight can be gained by viewing disordered materials as polymeric.

The scattered intensity from a polymer coil, described by a random walk of Kuhn steps of length b, follows the Debye equation (Debye, 1947, 1945),

$$I(q) = 2G[e^{-x} - (1 - x)]/x^2, \qquad (1)$$

where q is defined as $4\pi\sin(\theta/2)/\lambda$, θ is the scattering angle and λ is the wavelength of the radiation. $x = q^2R_g^2$ and $R_g^2 = zb^2/6$, z is the number of Kuhn steps of length b in a random walk. G is a constant defined by the specifics of the chain composition and the concentration of chains. For dilute chains, $G = N_p n_p^2$, where N_p is the number of polymer coils in the scattering volume and n_p

© 1996 International Union of Crystallography
Printed in Great Britain – all rights reserved

is a contrast factor. For X-ray scattering, n_p is the number of excess electrons in a coil relative to the solvent, thus, $G = N_p(\rho_e V_p)^2$, where V_p is the volume of a particle and ρ_e is the electron-density difference between the coil or particle and the solvent. For more concentrated chains, G takes on more complicated forms, as is discussed in §7 below.

The Debye equation predicts an exponential decay in scattering at low angles where the scattering vector q is of the order of $2\pi/R_g$, and R_g is the radius of gyration for the polymer chain. At higher angles, the scattered intensity decays with a power law of -2. Deviations from the Debye equation in the power-law regime may reflect collapse or expansion of the Gaussian chain leading to a mass scaling that differs from that of an ideal random walk. Equation (1) is an exact description of one structural level for a Gaussian chain. That is, it describes a Guinier regime and an associated power-law regime for a mass fractal of dimension 2.

Equation (1) is restricted to polymer coils of mass fractal dimension 2 because a random walk was assumed in the description of the chain conformation. Several attempts have been made to obtain a simple function that can describe scattering from polymer coils of arbitrary mass-fractal dimension. Such an equation would describe swollen or partially collapsed coils and branched polymers. An exact calculation of a Debye-like equation for arbitrary polymeric mass-fractal scaling was attempted by Benoit (1957) and by Peterlin (1953). Integral forms were obtained. A simple function suitable for curve fitting, however, was not obtained. An asymptotic expansion that applies in the high-q power-law scaling regime was described by Benoit.

Here, this asymptotic expansion of the integral form described by Benoit and Peterlin will be used to obtain the power-law prefactor for arbitrary mass-fractal dimensions. This expansion can be used in conjunction with the unified approach (Beaucage, 1995; Beaucage & Schaefer, 1994; Beaucage, Ulibarri, Black & Schaefer, 1995; Ulibarri, Beaucage, Schaefer, Olivier & Assink, 1992; Hua, Anderson, Hareid, Smith & Beaucage, 1994; Schaefer, Pekala & Beaucage, 1995) to describe scattering from polymeric mass fractals of arbitrary dimension. The unified equation under 'polymeric constraints' to the power-law prefactor can be used as a close approximation for (1) when the mass-fractal dimension deviates from 2. For example, it can be substituted for the Debye equation in the RPA (random phase approximation) equation for polymer blends (de Gennes, 1979). Equation (1) uses two independent parameters. The constrained unified equation uses three, the third being the mass-fractal dimension, d_f.

Besides a description of a single structural level, the unified approach can be easily extended to describe any number of related structural levels in a material, given a wide enough range of experimentally observed size. Two structural levels are present in a polymer coil. The large-scale structural level pertains to the chain's radius of gyration and the power law -2 regime as described by (1). At high q, the persistence length limits the mass-fractal scaling regime. Conventionally, the persistence length for the coil is described as a rod substructure. In the scattering pattern, the rod substructure is characterized by a Guinier regime for the average overall size of the rod and an associated power-law -1 regime that accounts for one-dimensional rods. These two structural levels can be consistently modeled using the unified approach.

Two structural levels are also present in broad classes of disordered materials. In analogy to a polymer chain, a large-scale structure is present that displays a mass-scaling regime at intermediate q. At high q, the substructure to the mass-fractal morphology limits the mass-fractal power law. Often, the substructure is a three-dimensional level with a power law described by Porod's law or surface-fractal scaling laws (Schmidt, 1992), in contrast to the one-dimensional rod substructure conventionally used for organic polymers.

Materials that can be described using the unified approach under polymeric constraints are termed 'polymeric mass fractals' here. Polymeric mass fractals can be distinguished from materials that are not polymeric but display power-law scattering with power-law slopes shallower than -3 by comparison of the power-law prefactor. Randomly oriented rods and lamellae are examples of these apparent mass fractals.

Several examples from polymer blends, far from the critical point, are examined where fits based on the unified equation under polymeric constraints are expected to be good. Additionally, examples from low-density silica aerogels are examined in which polymeric mass-fractal scaling that differs from a random walk is observed. The constrained unified approach works well in both cases. An example of an apparent mass fractal that does not follow the Benoit scaling function for polymeric mass fractals is also shown. For the case of a porous polymer-like system such as a nano-porous silica aerogel, the surface area per gram of the sample is calculated using the ideas presented here. The surface area of an apparent mass fractal is also calculated for comparison.

2. Unified Guinier-exponential/power-law equation

The unified equation (Beaucage, 1995) is an approximate form that describes a complex morphology over a wide range of q in terms of structural levels. A structural level in scattering is described by Guinier's law and a structurally limited power law, which on a log–log plot is reflected by a knee and a linear region (Figs. 1, 2 and 3). The approach can closely duplicate exact calculations for mass fractals, discussed here, and particles that display Porod behavior, as well as structures such as rods and

lamellae that display multiple structural levels (Beaucage, 1995). Moreover, the unified equation has been successfully applied to a number of experimental systems (Beaucage & Schaefer, 1994; Beaucage, Ulibarri, Black & Schaefer, 1995; Ulibarri, Beaucage, Schaefer, Olivier & Assink, 1993; Hua, Anderson, Hareid, Smith & Beaucage, 1994; Schaefer, Pekala & Beaucage, 1995). The unified equation for one structural level is given below.

$$I(q) \simeq G\exp(-q^2R_g^2/3) + B(1/q^*)^P, \qquad (2)$$

where $q^* = q/[\mathrm{erf}(kqR_g/6^{1/2})]^3$, G is the Guinier prefactor defined above and B is a prefactor specific to the type of power-law scattering. B is defined according to the regime in which the exponent P falls. Generally, for surface fractals $4 > P > 3$, for mass fractals $P < 3$ and for diffuse interfaces $P > 4$ (Schmidt, 1992; Korberstein, Morra & Stein, 1980; Debye, Henderson & Brumberger, 1957; Fischer & Burford, 1967). For Porod's law, $P = 4$ and $B = N_p 2\pi\rho_e^2 S_p$, where S_p is the particulate surface area. For a Gaussian polymer, $P = 2$, and B is given by $2G/R_g^2$, (5), through a comparison with (1) at the high-q limit as discussed below.

The constant, k, used to define q^* in (2), accounts for an approximation involved in the description of the low-q power-law limit (Beaucage, 1995). This is an empirical constant that has a value of 1 for steep power-law decays, $P > 3$. For weak power-law decays, k deviates slightly from 1. For polymeric mass fractals of fractal dimension d_f close to 2 (1.5 to 3), k is empirically found to be close to 1.06. Weak deviations are observed between the scattered intensity as calculated using (2) and exact calculations for values of q between $2\pi/R_g$ and π/R_g in these cases when $k = 1$. These deviations are reduced to less than 3% of the calculated intensity using $k = 1.06$.†

3. Polymeric structures of arbitrary mass-fractal dimension

3.1. *Radius of gyration, R_g, and $q = 0$ intensity, G*

The parameters G, R_g and B in (2) remain to be determined for a mass fractal of arbitrary mass-fractal dimension d_f. R_g for a polymeric mass fractal of dimension d_f is given by

$$R_g^2 = b^2 z^{2/d_f}/(1 + 2/d_f)(2 + 2/d_f). \qquad (3)$$

Equation (3) is obtained through incorporation of mass scaling behavior into the definition of R_g.‡ b is the Kuhn step length (Kurata & Tsunashima, 1989;

† From Beaucage, 1995, a value close to the empirically observed $k = 1.06$ can be obtained by integration $\int_0^{R_g} [\sin(qr)/q^*r] - [\sin(q^*r)/q^*r]\,dr \simeq 0$ for $k = 1.0497$. This means that with $k \simeq 1.05$ positive and negative deviations from the actual and approximated forms for the power-law cutoff at low q near R_g are balanced in the $q = 2\pi/R_g$ to $q = \pi/R_g$ region. The optimal value for k depends on $\gamma_0(r)$ and d_f but is expected to be close to 1.05, where $\gamma_0(r)$ is the correlation function.

‡ Equation (3) can be obtained by substitution of $R^2 = z^{d_f/2}\,b^2$ in the calculation of the radius of gyration, where R is the end-to-end distance for a polymer coil of fractal dimension d_f. For example, Heimenz (1984) gives a derivation of $R_g^2 = zb^2/6$ for a Gaussian coil. In Heimenz's book, l is substituted for b. If $k^{2/d_f}l^2$ is substituted for kl^2 in equation (1.56) of Heimenz, (3) results after the two indicated integrations are performed. For a rod, $d_f = 1$ and (3) leads to $R_{g,\mathrm{rod}} = R_{\mathrm{rod}}/12^{1/2}$, where $R_{\mathrm{rod}} = zb$. For a Gaussian coil, $d_f = 2$ and $R_{g,\mathrm{Gaussian}} = z^{1/2}b/6^{1/2}$.

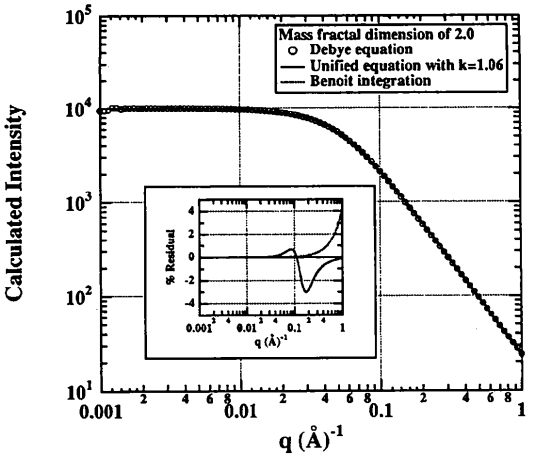

Fig. 1. Plot of log of calculated intensity *versus* log q from equations (1) and (2) for a Debye coil of $R_g = 71$ Å and $G = 10\,000$. The Benoit/Peterlin integral form is shown for comparison (dotted line). In the main figure, the dotted line overlaps with equation (2). Residuals as a percentage of equation (1) are shown in the inset. Deviations at high q for the B/P integral are due to a limited number of numerical integration steps.

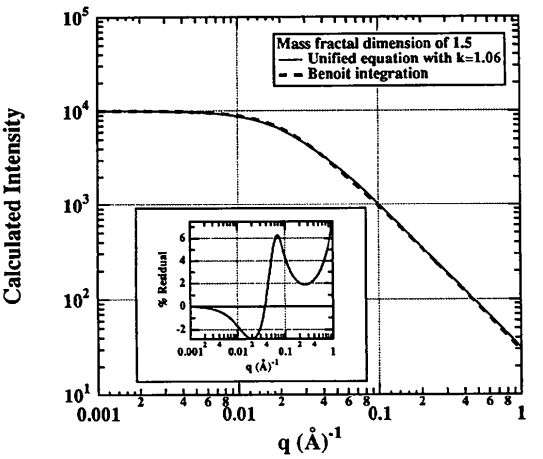

Fig. 2. Comparison of equations (6) and (2) for a polymeric mass fractal of $d_f = 1.5$, $R_g = 70$ Å and $G = 10\,000$. Residuals as a percentage of equation (6) are shown in the inset. The rise of residuals at high q is due to the limited number of numerical integration steps in equation (6).

Tsvetkov & Andreeva, 1989; Schmitz, 1990) and z is the number of Kuhn steps in the polymer chain. For an ideal chain, $d_f = 2$. G in (2) with dilute chain concentrations is given by

$$G = N_p \rho_e^2 V_p^2, \tag{4}$$

as noted above.

3.2. *Power-law prefactor, B*

For $d_f = 2$, the power-law prefactor B is given by

$$B = 2G/R_g^2 \quad \text{(for theta conditions)} \tag{5}$$

as noted above. This is a polymeric constraint to B for the special case of a Gaussian coil of fractal dimension 2. Under this constraint, (1) and (2) are compared in Fig. 1. A close agreement between the Debye equation and the unified equation is observed. Deviations at $q \simeq \pi/R_g$ are approximately evenly spaced about the calculation for (1). Thus, (2) constrained by (5) can approximate the Debye equation for polymer coils using the same two parameters, R_g and G. ($P = d_f = 2$ for the Gaussian coil.)

Benoit (1957) demonstrated that an exact non-integral function to describe arbitrary mass-fractal scaling cannot be obtained using the approach of Debye (1947, 1945). However, an integral form for arbitrary mass-fractal dimension is possible. Benoit's (1957) integral form is given by

$$I(q) = G\frac{d_f}{(qR_g)^{d_f}} \int_0^{(qR_g)^2} \left[1 - \frac{y^{d_f/2}}{(qR_g)^{d_f}}\right] e^{-y} y^{(d_f/2-1)} \mathrm{d}y. \tag{6}$$

Numerical integration of (6) can be used to calculate scattering from an arbitrary polymeric mass fractal. The integral can only be numerically solved and cannot be used to fit data except by iteration. For very small qR_g, (6) yields G, which is the Guinier prefactor previously described. For large qR_g, an asymptotic form is written (Benoit, 1957)

$$I(q) \underset{\text{high-}q}{\simeq} G\frac{d_f}{(qR_g)^{d_f}} \Gamma(d_f/2) - \ldots, \tag{7}$$

where Γ is the gamma function. By comparison with (2) the power-law prefactor is given by

$$B = (G\, d_f/R_g^{d_f})\Gamma(d_f/2) \tag{8}$$

for an arbitrary polymeric mass fractal. For $d_f = 2$, (8) yields (5) for the power-law prefactor. Equation (8) defines B in terms of G, R_g and d_f, thereby reducing the number of free parameters in the unified equation to three. This assumption is termed a 'polymeric constraint' on the unified equation.

Equation (2), using (3), (4) and (8), is compared with numerical integrations using (6). This comparison is done for $d_f = 2$ in Fig. 1, for $d_f = 1.5$ in Fig. 2 and for $d_f = 2.5$ in Fig. 3. The residuals shown in the lower left corner are as a percentage of (1) for Fig. 1 and (6) for Figs. 2 and 3. At high q, the integral form, (6), deviates from the actual power law owing to the limited number of steps in the numerical integration. For Figs. 1 and 3, 10 000 integration steps are used. For Fig. 2, 100 000 steps are used. The constrained unified equation uses three unknown parameters including d_f. Equation (1) uses two unknown parameters with d_f fixed at 2.

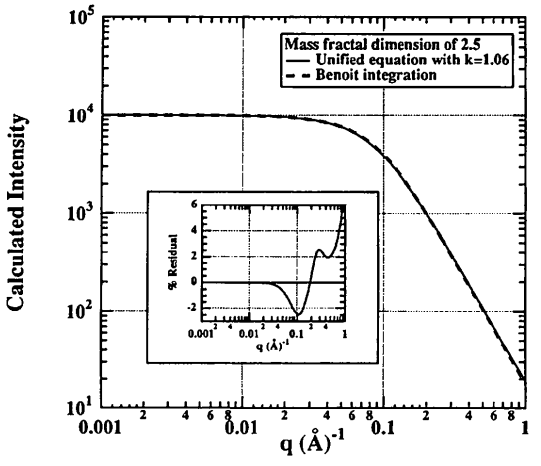

Fig. 3. Comparison of equations (6) and (2) for a polymeric mass fractal of $d_f = 2.5$, $R_g = 42$ Å and $G = 10\,000$. Residuals as a percentage of equation (6) are shown in the inset. The rise of residuals at high q is due to the limited number of numerical integration steps in equation (6).

4. A high-q cutoff for power-law scattering and the unified equation

The unified equation can be used to calculate scattering from an arbitrary number of structural features at different sizes if a sufficient range of size is observed. For example, the transition from power-law -2 scaling for a polymer chain to power-law -1 for the rod-like Kuhn steps of a chain can be easily described. This is done by considering two structural levels, a large structural level corresponding to the chain, which is composed of a small structural level, the rod subunits corresponding to Kuhn steps. In this case, the high-q power-law prefactor for a dilute suspension of randomly oriented rods is known from classic work (Guinier & Fournet, 1955) to be $N_r n_r^2 \pi/2L$, where L is half the Kuhn-step length (Kurata & Tsunashima, 1989; Tsvetkov & Andreeva, 1989; Schmitz, 1990), N_r is the number of rods in the scattering volume and n_r is the number of electrons per rod; for X-ray scattering, $n_r = \rho_e V_{\text{rod}}$, where ρ_e is the skeletal electron density of the chain. The skeletal electron density of the chain is the electron density of the rod-like Kuhn step. V_{rod} is the corresponding volume per Kuhn step. n_r can also be approximated using Bondi's method of group contribution (Bondi, 1964; Beaucage & Stein, 1993*a*) or using molecular-modeling software.

In the unified approach, an exponential prefactor is used to describe the high-q structural limit for fractal scaling (Beaucage, 1995; Beaucage & Schaefer, 1994; Beaucage, Ulibarri, Black & Schaefer, 1995; Ulibarri, Beaucage, Schaefer, Olivier & Assink, 1992; Hua, Anderson, Hareid, Smith & Beaucage, 1994; Schaefer, Pekala & Beaucage, 1995). The two size limits to mass-fractal scattering for a polymer coil are described through an extension of (2).

$$I(q) \simeq G\exp(-q^2R_g^2/3) + B\exp\left(\frac{-q^2R_{\rm sub}^2}{3}\right)\left(\frac{1}{q^*}\right)^P + G_s\exp\left(\frac{-q^2R_s^2}{3}\right) + B_s\left(\frac{1}{q_s^*}\right)^{P_s}, \quad (9)$$

where $q^* = q/[\mathrm{erf}(qkR_g/6^{1/2})]^3$ and $q_s^* = q/[\mathrm{erf}(qk_sR_s/6^{1/2})]^3$. Equation (9) is developed by Beaucage & Schaefer (1994). The first term in (9) describes the large-scale polymer coil of size R_g composed of small-scale Kuhn steps of size R_s, captured in the third term. The second term describes the mass-fractal regime with two structural limits. The low-q limit is at R_g and is described by the error function. The high-q limit is at $R_{\rm sub}$ and is described by the exponential prefactor (Beaucage, 1995). The final two terms are (2) for the substructural mer unit. Using (9), scattering from a system with multiple-size-scale features is parameterized. Generally, the high-q cutoff for the intermediate power law, $R_{\rm sub}$, is identical to the substructural radius of gyration, R_s. The assumption that $R_{\rm sub} = R_s$ should always be true for typical mass fractals. It should be noted that, although (9) appears cumbersome, no new parameters have been introduced over local fits using exponentials and power laws. Under the assumption that $R_{\rm sub} = R_s$, (9) can be extended to describe an arbitrary number of interrelated structural features at different size scales,

$$I(q) \simeq \sum_{i=1}^{n}\left[G_i\exp\left(\frac{-q^2R_{gi}^2}{3}\right) + B_i\exp\left(\frac{-q^2R_{g(i+1)}^2}{3}\right)\left(\frac{1}{q_i^*}\right)^{P_i}\right], \quad (9')$$

where $i=1$ refers to the largest size structure and $q_i^* = q/[\mathrm{erf}(qk_iR_{gi}/6^{1/2})]^3$. Such extensions, however, can only be justified when data extend over many decades in q. Again, (9′) introduces no new parameters over local Guinier and power-law fits.

For a polymer coil we consider a special case in which P_s in (9) is often assumed to be 1 for a rod-like Kuhn step and B_s is given by equations for rod scattering (Guinier & Fournet, 1955),

$$B_{\rm rod} = \frac{N_p n_{\rm rod}^2 \pi}{2R}. \quad (10)$$

$R = R_{\rm sub} = R_s$ is defined by the Kuhn-step length, $n_{\rm rod}$ is the number of electrons per Kuhn step and N_p is the number of Kuhn steps in the scattering volume.

Equations (9) and (9′) are most useful in systems where structural levels are well separated in size such as in polymer coils and simple mass fractals. If different structures of similar size exist in a material, the unified approach can be used to separate contributions to scattering, but this depends on the resolution of the data. Miscible polymer–polymer blends are a special case. Such blends can be dealt with using the RPA approach of de Gennes coupled with either (2) or (9) or (9′). This manuscript demonstrates that (2) is a good approximation for the Debye equation used in the RPA approach when the mass-fractal dimension deviates from (2). In a publication to follow, application of the unified approach to polymer blends will be dealt with in detail.

5. Applications of polymer functions to disordered materials

The description of polymeric mass fractals is applicable to a number of systems that are not generally considered polymers. For example, polymerization phenomena in the formation of silica based aerogels leads to power-law scattering with power-law slope −2.5. Scattering from this disordered material obeys the unified equation under polymeric constraints discussed above. Several cases are summarized in Table 1.

In all the experimental cases we have investigated (Beaucage & Schaefer, 1994; Beaucage, Ulibarri, Black & Schaefer, 1995; Ulibarri, Beaucage, Schaefer, Olivier & Assink, 1992; Hua, Anderson, Hareid, Smith & Beaucage, 1994; Schaefer, Pekala & Beaucage, 1995), mass-fractal scattering can be described by three parameters, R_g, G and d_f, using the unified equation, (2) and (9), under polymeric constraints, (8). This description is true for all the materials in Table 1 except the low-dimensional objects. For materials that display a weak power-law decay but are not mass fractals, such as randomly oriented rod and lamellar systems, this approach leads to a mismatch between the observed (Beaucage & Schaefer, 1994) or calculated intensity (Beaucage, 1995) and the unified equation under polymeric constraints. The unified equation can still be used but with B calculated for that particular structure (Beaucage, 1995; Beaucage & Schaefer, 1994) as discussed in §6 below.

In the disordered-materials field, nanoporous materials with a mass-fractal morphology are occasionally encountered. Examples of such materials include fumed silica (Beaucage, Ulibarri, Black & Schaefer, 1995), tetraethoxysilane and tetramethoxysilane based aerogels and zerogels (Beaucage & Schaefer, 1994), colloidal-silica-based aerogels (Hua, Anderson, Hareid, Smith & Beaucage, 1994) and several cases of low-density

Table 1. *Several cases of mass-fractal power-law scattering (modified from Schaefer, Martin & Keefer, 1985)*

Mass-fractal structures	Power-law slope
Polymers	
Polymer in good solvent	−1.5
Self-avoiding walk (linear swollen polymer)	−1.67
Random walk (polymer in theta solvent)	−2.0
Swollen branched polymer	−2.0
Randomly branched ideal polymer	−2.29
Non-equlibrium growth processes	
Multiparticle diffusion limited aggregate	−1.8
Percolation cluster	−2.5
Diffusion limited aggregate	−2.5
Low-dimensional objects (apparent mass fractals)	
Randomly distributed rods	−1.0
Randomly distributed lamellae or platelets	−2.0

polymer foams such as some of the resorcinol-formaldehyde aerogels (Schaefer, Pekala & Beaucage, 1995). In these cases, it is desirable to have a method by which the surface area can be determined from the mass-fractal scaling regime of the small-angle scattering pattern. The surface area can be estimated by application of the polymer model, discussed above, to these materials. Generally, the surface area is expected to vary with the size scale of observation, which corresponds to the size scale of the molecular probe used in a gas absorption experiment, for example. In a scattering experiment, the size scale of observation varies with $2\pi/q$. Scattering offers the opportunity to measure the scaling of surface area with the size scale of observation. Observing a mass fractal at size scale $2a$ is equivalent to considering a chain structure composed of subunits of size $2a$. This subunit may correspond to a Kuhn step of the chain if the size of observation is the same as that of a Kuhn step. Often the size scale of interest, however, is defined by a technique such as gas absorption* (Hurd, Schaefer, Smith, Ross, Le Mehaute & Spooner, 1989), yielding an arbitrary size scale $2a$ that is not related to the chains Kuhn step.

The scaling relationship between the surface area and the size scale of observation, $2a$, can be determined by consideration of the surface area per chain. The chain might be approximated by a spherical structure whose size scales with the chain's radius of gyration. Such a chain can be thought of as being composed of subunits of arbitrary size, smaller than the chain's radius of gyration. These subunits of smaller size could be approximated as spheres whose sizes are related to the subunit's radius of gyration. Because the subunits are arbitrary sections of the chain, their structure is mass fractal. These arbitrary subunits are composed of Kuhn-step units, as shown in Fig. 4. In this approach, the mass-fractal scaling of a subunit matches the mass-fractal scaling of the chain (note the self-similarity between the chain and the arbitrary subunit of Fig. 4). The overall surface area per coil is $N_{2a}S_{\text{sub}}$. N_{2a} is obtained from R_g using (3) and $b=2a$.

$$N_{2a} = (1+2/d_f)^{d_f/2}(2+2/d_f)^{d_f/2}(R_g/2a)^{d_f}. \quad (11)$$

Thus, for a spherical unit:

$$S_{\text{coil}} = K_{\text{sph}} R_g^{d_f} a^{2-d_f}, \quad \text{spherical unit,} \quad (12)$$

where $K_{\text{sph}} = 4\pi 2^{-d_f}(1+2/d_f)^{d_f/2}(2+2/d_f)^{d_f/2}$. To reiterate, in (11) and (12), a is an arbitrary size in the mass-fractal scaling regime that is fixed by the size scale of observation. When one is comparing scattering data to a measurement with a fixed size scale of observation, such as a gas absorption measurement, the size scale of the comparative technique is used. Because the mass of a coil is fixed, the surface area per coil given by (12) is proportional to the specific surface area for the sample, *i.e.* the surface area per mass. This is related to the surface area per volume through the sample density. The mass per coil, although constant, is sometimes difficult to determine if the mass per Kuhn step or mass per persistance segment length is not known. If the mer units are observed in the scattering pattern, this problem can be overcome, as is discussed in §7.2 below.

In (12) the surface area per coil increases with decreasing a for $d_f > 2$. For $d_f = 2$, the coil surface area does not depend on the size scale of observation, a. For $d_f < 2$, (12) predicts a decreasing coil surface area with decreasing a. Equation (12) can be viewed as a design criterion for materials of high surface area based on three rules. (i) If high surface area is desired from a mass-fractal material, (12) indicates that a mass-fractal dimension greater than 2 is necessary. (ii) Moreover, (12) defines a Gaussian mass fractal composed of spherical subunits as one in which the surface area does not change with size scale of observation. (iii) Mass fractals that display a dimension less than 2 are predicted to display the peculiar and nonintuitive behavior of a decreasing surface area with size scale of observation. This behavior is because the radius of the chains' primitive path (de Gennes, 1979) decreases with size of the spherical subunits.

Point (iii) can be clarified by consideration of the structure of an arbitrary coil subunit for $d_f < 2$. Equation (12) is obtained by considering each subunit to obey the same scaling as the polymer coil as a whole. The subunits

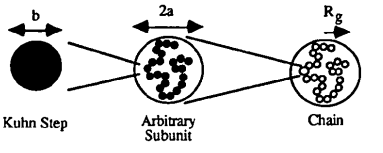

Fig. 4. A mass-fractal chain composed of subunit chains of arbitrary size that are in turn composed of Kuhn steps. The size of the subunit chains corresponds to the size scale of observation.

* The idea of two conditions for the substructural size is also important to the determination of surface area for surface fractals, as is shown in the last part of §7.

are considered to approximate spherical structures. Alternatively, the polymer coil can be considered to be composed of subunits that have some degree of asymmetry. This asymmetry might be rooted in the chemical composition of a subunit for the chain. Mass-fractal scaling with a dimension less than 2 might indicate a stiffer or more rod-like chain. Under these conditions, the assumption that the subunit is a sphere may not be appropriate. A more appropriate assumption might be to use a rod with some aspect ratio. For a rod subunit with radius c and length $2a$, the surface area per coil is given by

$$S_{\text{coil}} = N_a(2S_{\text{rod end}} + S_{\text{rod side}}) = K_{\text{rod}} R_g^{d_f}[(2a)^{-d_f} c^2 + c(2a)^{1-d_f}], \quad \text{rod-like unit,} \tag{12'}$$

where $K_{\text{rod}} = 2\pi\,(1 + 2/d_f)^{d_f/2}\,(2 + 2/d_f)^{d_f/2}$. Equation (12′) leads to a dependence of coil surface area with size of measurement a more consistent with intuition* for fractal dimensions smaller than 2. If the rods are connected at their ends, the contribution of the rod end term, first term in (12′), will be diminished. Additionally, the rod diameter, c is expected to scale in some way with the size of observation, a. Equation (12) is expected to be obeyed close to the chain radius of gyration, low q, while (12′) is expected to be obeyed close to the Kuhn-step size, expecially for rod-like Kuhn steps.

When the scattering pattern is measured over a sufficient range of q to observe the substructural units of the chain (Kuhn steps), the two structural levels of the chain can be fitted using (9). Surface fractal or Porod approaches can then be used to determine the surface area for the chain's substructural units (Kuhn steps). In order to calculate the surface area, the volume of the substructural unit needs to be determined. The volume of the mer unit can be obtained by separating the part of the fit pertaining to the subunit, the second two terms in (9). The calculated curve from this part of the fit multiplied by q^2 can be integrated to obtain the Porod invariant, Q, for the substructure, without scattering from the large-scale mass-fractal morphology, according to (15) below. The volume of a mer unit can be obtained from Q and G. Assuming a model for the substructure such as a rod or sphere, one can obtain a second value for the volume of the mer unit using the radius of gyration for this substructure measured in the data at high q. If the two values for the volume of the subunit agree, the model is acceptable. This model can be used to calculate the surface-to-volume ratio for a mer and the specific surface area for the microporous sample. This approach is used in §7.2 below.

* Since $d_f = 1$ is the lowest dimension for a chain to show increasing surface area with decreasing size of measurement, this is the lowest dimension allowed in the polymer model. Moreover, the term $[1 - y^{d_f/2}/(qR_g)^{d_f}]$ in (6) limits d_f to values greater than 1.

When the mer subunit to polymeric scattering is observed in the scattering pattern, it should be compared to the size of a comparison technique, *e.g.* gas absorption. If the comparable measurement size $2a$ falls in the polymeric mass-fractal scaling regime, that is $2a > b$, then the scaling relationships, (12) above, are appropriate for the determination of surface area, Fig. 9 below. When $2a < b$, the surface area should be obtained from the high-q surface-fractal scaling regime using the Porod or surface-fractal approach (Hurd, Schaefer, Smith, Ross, Le Mehaute & Spooner, 1989; Bale & Schmidt, 1984; Wong & Bray, 1988) if sufficient data are available in this regime. The surface area can be approximated for a polymeric mass fractal even when $2a < b$. This approach is used to determine the surface area of Airglass® in §7.2 below and is compared to the value obtained using the surface-fractal approach.

6. Low-dimensional objects (apparent mass fractals)

As noted above (Table 1), a number of systems display mass-fractal-like power-law scattering, that is power-law decays shallower than -3, yet do not fit into the structural category of polymeric mass fractals. For example, a power law of -2 is expected from randomly oriented lamellae. Such materials, which do not follow the Benoit/Peterlin power-law prefactor, (8), will be termed 'apparent mass fractals'. The power-law prefactor for these materials is expected to follow classic functions. For a dilute suspension of lamellar particles:

$$B_{\text{lam}} = N_p 2n^2/R^2, \tag{13}$$

where $2R$ is the long dimension of the lamella and $P = 2$ (Guinier & Fournet, 1955) in (9). For rod systems, (10) applies and $P = 1$.

By conservation of units and by comparison with the power-law prefactors for lamellar and rod systems, a generalized form for the power-law prefactor of apparent mass fractals is obtained:

$$B_{\substack{\text{apparent} \\ \text{mass-fractal}}} = AN_p\rho_e^2 S_p r^{(4-d_f)} = AG(S_p/V_p^2) r^{(4-d_f)}, \tag{14}$$

where A is a unitless geometric factor, V_p is the volume of one low-dimensional particle, S_p is the surface area per particle and r is the small dimension of the particle such as the radius of a rod or half the thickness of the lamella. For a lamellar system, $A = 4\pi$ and $d_f = 2$. For a rod system, $A = \pi^2/2$ and $d_f = 1$. In the majority of cases, the structure is not an ideal lamella or rod so the small dimension, r, is not easily determined. For these cases, it is simpler to substitute the high-q cutoff to the apparent-mass-fractal regime in terms of the high-q radius of gyration measured in the scattering pattern, R_{sub} of (9), for r in (14) and to include all structural factors in the unknown constant A. For lamellae and rod systems, we can compare the classic exponential cutoff given by Guinier

& Fournet (1955) with the power-law cutoff, $e^{-iR_g^2q^2/3}$, of (9), to obtain A (Beaucage, 1995). When the power-law cutoff, R_{sub} of (9), is used for r, A for a rod is $4\pi^2/3^{3/2}$ and A for a lamella is 4π.

Using (14), we can explore structures that deviate from ideal rods or ideal lamellae. The Porod invariant, Q, can be used to simplify (14):

$$Q = \int_0^\infty I(q)q^2\,dq = 2\pi^2 G/V_p \tag{15}$$

$$B_{\substack{\text{apparent}\\ \text{mass-fractal}}} = [AQ(S_p/V_p)/2\pi^2]r^{(4-d_f)}. \tag{16}$$

G, d_f and Q can be obtained from the scattering pattern (d_f is the negative of the power-law slope). r is given by the observed limit to apparent-mass-fractal scaling at high q using a unified fit, (9), as discussed above. Equation (16) can be used to obtain the particulate surface-to-volume ratio, S_p/V_p, multiplied by the geometric factor, A. As noted above, A is expected to be between 7.6 and 12.6. Assuming a value for A, one can obtain the specific surface area from

$$\frac{\text{total surface area}}{\text{mass sample}} = \frac{(S_p/V_p)\varphi_p}{\rho_{sam}} = \frac{2\pi^2\varphi_p B_{\substack{\text{apparent}\\ \text{mass-fractal}}}}{A\,\rho_{sam}Qr^{(4-d_f)}} \tag{17}$$

where ρ_{sam} is the sample density and φ_p is the volume fraction of structures in the sample. For a nano-porous material, φ_p can be obtained from the density of the sample.

7. Results/discussion

7.1. *Polymer blends far from the critical point*

In Fig. 5, neutron scattering from a symmetric (matched molecular weights, 50:50 blends), isotopic (H/D) polystyrene blend at 399 K is fitted. The incoherent background was independently measured and subtracted from the data. The interaction parameter, χ, for this case is negligibly small. Since the sample is somewhat polydisperse ($M_w/M_n \simeq 1.3$), the degree of polymerization (DOP) is allowed to float in the fit. The prefactor, G, is calculated in this case as $G = \text{DOP}\ V_{mer}\ \varphi_{vH}\varphi_{vD} \times (\rho_H - \rho_D)^2 = 0.1055$ DOP cm^{-1}, where φ_{vi} is the volume fraction of component i, ρ_i is the neutron scat-tering density for a mer unit of type i and V_{mer} is the volume of a mer unit, that is, the molar volume divided by Avagadro's number. This equation is from the RPA equation (de Gennes, 1979) using $\chi = 0$ and equal degrees of polymerization and molar volumes for the blend components. The radius of gyration is also calculated from (3) with knowledge of the statistical segment length of 6.8 Å for PS, the DOP and d_f. Conventional RPA fits are limited to the first 10 to 15 data points and therefore ignore deviations in mass-fractal scaling. That is, the conventional fit range excludes the power-law regime. Here, the entire data set is fitted to the Debye equation, (1), using only the DOP as a parameter. (R_g is fixed by (3) using $d_f = 2$.) The DOP from the Debye fit is 4040. The Debye equation (with d_f fixed at 2) leads to a poor fit (dashed line in Fig. 5). When d_f is also used as a free parameter in (2) under polymeric constraints (8) the data are matched extremely well for $d_f = 2.11$ and DOP = 2400. The weight average DOP for this blend from gel permeation chromatography is 2210. Allowing the fractal dimension to vary slightly accounts for deviations in the data from Gaussian behavior.

The third fit in Fig. 5 uses the same parameters as the least-squares two-parameter fit to (2) and (8). Moreover, it includes parameters from a local fit to the high-q data with a power law of -1 for rod behavior using (9). A radius of gyration of 6.3 Å is used for the high-q regime. This value is obtained by calculation of the radius of gyration of a rod whose length is the persistence length of polystyrene, 12.41 Å (Kuhn length/2), and whose radius is 7.3 Å. The radius is obtained from molecular models (Beaucage, Stein & Koningsveld, 1993; Beaucage & Stein, 1993). Since only limited data are available for this regime, the fit is only meant to demonstrate the ability of the unified approach to model transitions between structural levels as discussed above.

When some degree of swelling or collapse of the coils is present, (2) and (9) may be useful as substitutes for the Debye equation in the random-phase approximation (de Gennes, 1979) to determine the interaction parameter for polymer blends. Additionally, (9) can account for deviations from the Debye equation at high q for rigid systems where segment structure overlaps with Debye scattering.

Fig. 5 can be compared with Fig. 6. In this case, an isotopic blend of polydimethylsiloxane is shown. The

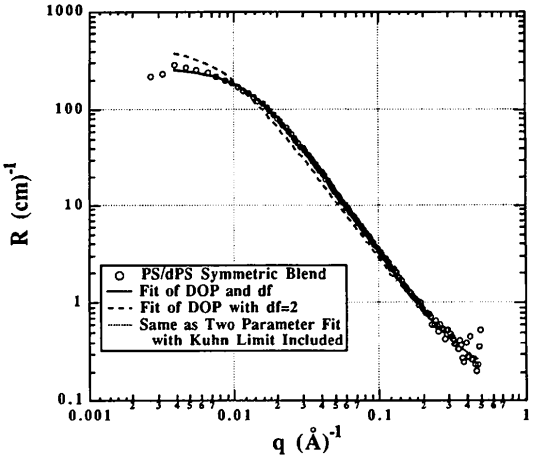

Fig. 5. log R, absolute intensity (or Rayleigh ratio), *versus* log q for neutron scattering data from a symmetric isotopic blend of polystyrene at 399 K. Fits are to equations (1), (2) and (9) as discussed in the text. The incoherent background has been measured and subtracted from these data.

data do not display deviations from Gaussian behavior for this flexible chain. Additionally, since the calculated radius of gyration for the rod subunit, 3 Å [based on the persistence length of 7.35 Å and an estimated radius of 3.15 Å from the Bondi approach (Bondi, 1964)], is just outside the observable range for the data, the Debye equation fits the data even at very high q.

Finally, we can consider a polymer blend with specific interactions. Fig. 7 shows neutron scattering data from a PVME/dPS blend (polyvinylmethylether/deuterated polystyrene) in which the PVME has a high degree of isotacticity (Beaucage & Stein, 1993*b*). The mass-fractal dimension using the unified fit under polymeric constraints is 1.8. This deviation from $d_f = 2$ may be due to a good solvent effect. Blends with a higher percentage of PVME show stronger deviations from ideal behavior. For this blend, the high-q R_g is fixed at 6.8 Å and P for the high-q power law is fixed at 1 for rod-like scattering.

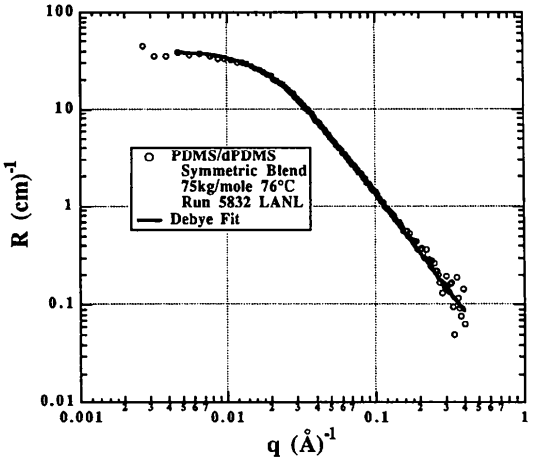

Fig. 6. Neutron scattering data from a symmetric isotopic blend of d-PDMS with PDMS. Data do not show deviations from $d_f = 2$ for molecular weights of 15, 25, or 75 kg mol^{-1} over temperatures from 273 to 373 K (75 kg mol^{-1} sample is shown.) The incoherent background has been measured and subtracted from these data.

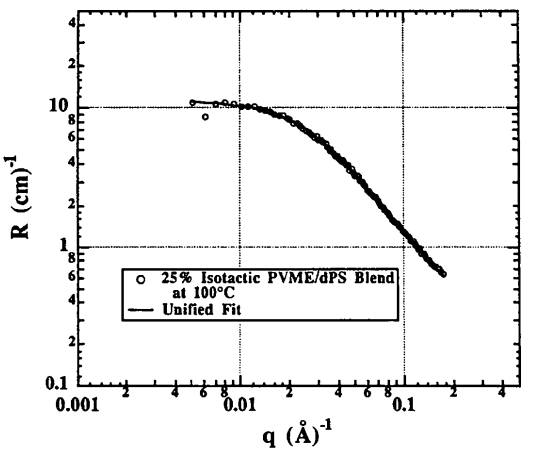

Fig. 7. Neutron scattering data from an isotactic PVME/dPS blend far from the critical point that shows deviations from Gaussian behavior. The fit is to the unified equation under polymeric constraints, equation (9), yielding $d_f = 1.8$, $R_g = 55$ Å. The incoherent background has been measured and subtracted from these data.

7.2. *Low-density silica aerogels*

A number of materials that would not normally be considered polymers display polymeric mass-fractal scaling. That is, scattering data from these systems can be fitted with the unified approach, (2) or (9), using polymeric constraints, (8). An interesting case is that of low-density nano-porous silica aerogels. Aerogels can be made by supercritical extraction of aqueous gels based on hydrolysis of tetraethoxysilane (TEOS) or tetramethoxysilane (TMOS). (A good review of silica aerogels can be found in Brinker & Scherer, 1990.) Variation of the pH of the gel precursor leads to dramatic variation in structure. A polymeric structure can result under the proper conditions of pH (Schaefer, Olivier, Ashley, Richter, Farago, Frick, Hrubesh, van Bommel, Long & Krueger, 1992; LeMay, Hopper, Hrubesh & Pekala, 1990). For silica aerogels, the most important material property is the small pore size that leads to high specific surface areas.

The polymeric mass-fractal approach is useful in using small-angle scattering to determine the surface area of nano-porous samples that display mass-fractal scaling. As discussed above, the determination of a surface area for a mass fractal requires the use of a model for the base structure, of Kuhn step in the polymeric structure. The base structure must be observed in the scattering pattern to determine an appropriate model.

Data from a commercial silica aerogel sample, Airglass®, are shown in Fig. 8. A polymeric mass-fractal

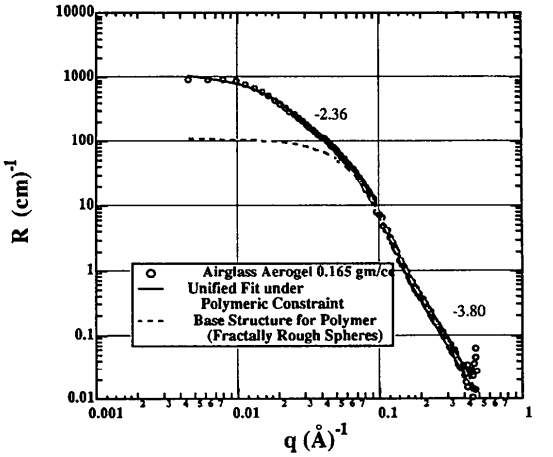

Fig. 8. X-ray scattering data from Airglass® silica aerogel. The high-q cutoff to mass-fractal scaling occurs close to the second decade line in q where the power-law slope shifts from −2.36 to −3.80. Unified fit is to equation (9) with $R_g = 107$ Å, $G = 983$ cm^{-1}, $B = d_f G\Gamma(d_f/2)/R_g^{d_f} = 0.0352$, $P = d_f = 2.36$, $R_{sub} = R_s = 30.2$ Å, $G_s = 107$ cm^{-1}, $B_s = 0.000768$, $P_s = 3.80$.

regime, $d_f = 2.36$, is observed in the second decade of q. That is, the data fit the unified equation under the polymeric constraint. This sample of Airglass® displays the two limits to polymeric mass-fractal scaling in the conventional small-angle X-ray scattering size regime. The low-q limit is a Guinier regime reflecting the coil-like radius of gyration of a chain structure, 107 Å, the low-q knee in the log–log plot of Fig. 8. The high-q limit is related to the Kuhn-step size for the chain-like structure (high-q knee in Fig. 8). Above the high-q limit, the base structure of the chain is observed. The base structure can be described as fractally rough particulates with surface-fractal dimension, $d_s = 6 - P_s = 2.2$, and with a radius of gyration of 30.2 Å.

The high-q part of the global fit (dotted line in Fig. 8), reflects the substructural mer unit in the absence of the low-q mass-fractal scaling regime. This curve is due to the second two terms of (9) and yields $G_{\text{high } q} = 107\ \text{cm}^{-1}$ and the invariant $Q = 0.0148\ \text{cm}^{-1}\ \text{Å}^{-3}$. (The invariant, Q, from the fit to the whole data set is $0.0193\ \text{cm}^{-1}\ \text{Å}^{-3}$.) From (15), the volume of the base structural unit is therefore 142 600 Å^3. We can use the high-q radius of gyration, 30.2 Å, to describe the base structural size, a. Using a spherical model for the base unit of the polymer chain with $r = R_s(5/3)^{1/2} = 39$ Å and $\rho_{\text{base structural unit}} = 2.2\ \text{g cm}^{-3}$, a degree of polymerization of 15 and a surface area of $610\ \text{m}^2\ \text{g}^{-1}$ are obtained. The volume of a sphere of radius 39 Å is 248 700 Å^3, which does not agree with the volume from the high-q invariant of 142 600 Å^3 given above.

Since the assumption of a hard-sphere base unit to the polymeric structure leads to this discrepancy in base unit volume, we consider an asymmetric structure, a rod, as the base for the polymeric structure. Since the data fail to show a power-law -1 regime at high q, the aspect ratio (ratio of the principle radii of the rod structure) must be less than 2.5 to 3 (Feigin & Svergun, 1987). The radius of gyration for a rod is given by $R^2_{g\,\text{rod}} = r^2/2 + R^2/3$, where r is the radius of the rod and R is half the length of the rod. For an aspect ratio of 2, $R = 44.6$ and $r = 22.3$ and the subunit volume = 139 700 Å^3 (DOP = 11*). This is very close to the correct aspect ratio for the base structure, since the calculated and measured particle volumes agree. Using these sizes, the surface area per gram is calculated to be $348\ \text{m}^2\ \text{g}^{-1}$ if only the sides of the rod are used to calculate surface area and $436\ \text{m}^2\ \text{g}^{-1}$ if the slides and ends are used to calculate the surface area, (12′). The surface area measured by nitrogen absorption is close to $500\ \text{m}^2\ \text{g}^{-1}$.

A second approach to surface area calculation is to consider the surface area of the surface-fractal base structure. The dotted line in Fig. 8 corresponds to this component of the unified fit, the last two terms of (9). The surface area for a surface fractal (Hurd, Schaefer, Smith, Ross, Le Mehaute & Spooner, 1989; Bale & Schmidt, 1984; Wong & Bray, 1988) at a size of measurement r is given by $S(r) = Sr^{2-d_s}$, where

$$S = 2\pi\varphi(1 - \varphi)B/Q\rho_{\text{sample}}F(d_s),$$

and

$$F(d_s) = \Gamma(5 - d_s)\sin[\pi(3 - d_s)/2]/(3 - d_s).$$

For the microporous material of Fig. 8, $\varphi = -\rho_{\text{sample}}/\rho_{\text{base material}} = 0.036$, where $\rho_{\text{sample}} = 0.08\ \text{g cm}^{-3}$ and $\rho_{\text{base material}} = 2.2\ \text{g cm}^{-3}$. B for the high-q power-law regime is $0.000768\ \text{cm}^{-1}\ \text{Å}^{6-d_s}$ and $F(d_s) = 1.99$. In order to calculate Q, (15), parameters from the high-q unified fit for the surface-fractal structure are used to simulate the scattering pattern of the base structure in the absence of the large-scale structure. This corresponds to the dashed line in Fig. 8. As noted above, integration of the dashed curve in Fig. 8 yields $Q = 0.0148\ \text{cm}^{-1}\text{Å}^{-3}$. A large-scale cutoff to the surface-fractal scaling regime is not observed in the

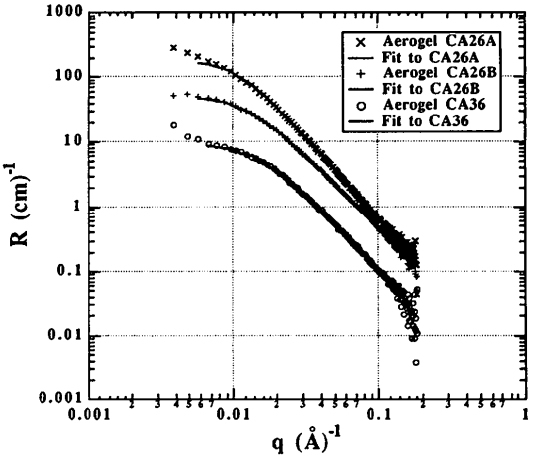

Fig. 9. log–log plot of neutron scattering data from a series of silica aerogels (data from D. W. Schaefer and C. S. Ashley) fitted to the unified equation under the polymeric constraint. For CA26A $R_g = 144$ Å, $d_f = 2.46$ and $G = 207\ \text{cm}^{-1}$, for CA26B $R_g = 119$ Å, $d_f = 2.24$ and $G = 54.6\ \text{cm}^{-1}$, and for CA36 $R_g = 99.2$ Å, $d_f = 2.34$ and $G = 9.94\ \text{cm}^{-1}$. Samples prepared by C. Ashley, Sandia National Laboratories.

* A DOP of 11 is based on the assumption that the substructure is a prolate ellipsoid aligned in the long direction along the chain axis. For a prolate ellipsoid aligned perpendicular to the chain, the DOP is 56. An oblate ellipsoid is also possible. Additionally, substructural polydispersity cannot be distinguished from asymmetry in the scattering pattern leading to further complication to this approach. However, as a simple model for the morphology, the approach presented here is satisfactory. An additional concern is the low DOP values. Most of the equations presented here are based on the large DOP limit which this sample of Airglass® probably does not meet. Airglass® is used as an example because the morphology is known to be polymer-like from electron micrographs and because the coil structure and the substructure can be clearly observed in the scattering pattern. Other low-density silica materials display a much higher DOP. Fig. 9, for example, shows three aerogels which have DOPs of the order of 1000 to 10 000 based on $2a = 5$ Å and (11). In these samples, the substructure is out of the observable size range.

data; the data go to $2\pi/q = 16$ Å. We can estimate that this cutoff size is close to the structural size of an SiO_2 unit which is 3 to 5 Å depending on the degree of substitution, from the Bondi (1964) method. Here $r = 4$ Å can be used following Hurd (Hurd, Schaefer, Smith, Ross, Le Mehaute & Spooner, 1989) for nitrogen absorption. We have $S(r) = 715\ r^{-0.2}$ and $S_{4\,A} = 542\ m^2\ g^{-1}$. This surface area is larger than the surface area for the polymeric structure, as is expected because the polymeric model assumed a smooth interface while this model accounts for surface roughness. The measured N_2 absorption Brunauer, Emmett & Teller surface area for this sample is close to 500 $m^2\ g^{-1}$, as noted above. Most of the surface area in the sample results from the polymeric mass-fractal nature of the sample. The surface-fractal characteristic of the base structure increases the total surface area by 20 to 36% depending on the portion of the rod subunit used to calculate the surface area.

For Airglass®, the base structure was observed in the scattering pattern and this was used to estimate a model for the subunit of the chain. This model was used to determine the surface area for the sample in the mass-fractal regime. Often, the base structure is not observed in the accessible range of q. Fig. 9 is an example of this type of neutron scattering data for three silica aerogels with polymeric mass-fractal structures. Fits to the unified equation under polymeric constraints are shown. These are three-parameter fits, G, R_g and d_f, using (2) and (8). The mass-fractal dimension varies from 2.2 to 2.5 in this series. The surface area for these structures might be estimated using the approach discussed above. In Fig. 9,

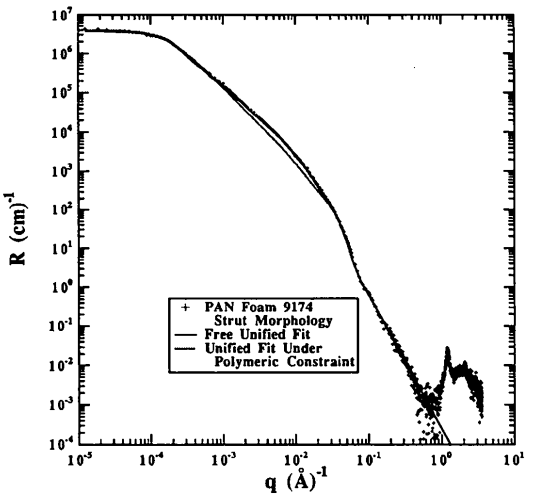

Fig. 10. Light scattering, Bonse–Hart X-ray data and conventional X-ray data on low-density polyacrylonitrile foam with a strut morphology, x. —— fit to equation (9) with $R_g = 8200$ Å, $G = 3.64 \times 10^6\ cm^{-1}$, $P = 1.61$, $B = 2.1\ cm^{-1}$, $R_{sub} = 120$ Å, $R_s = 66$ Å, $G_s = 410\ cm^{-1}$, $P_s = 3.391$, $B_s = 0.000243$; - - - - - unified fit under polymeric constraint, $P = 1.83$ from a least-squares fit. The constrained fit does not match the data in the third and fourth decades of q since the material is not a polymeric mass fractal.

the DOP for a substructure with $2a = 5$ Å is CA26A = 28 900; CA26B = 8140 and CA36 = 7640 from (11).

7.3. *Apparent mass fractals (low-density polymer foams)*

Fig. 10 is scattering data for a low-density microporous polyacrylonitrile (PAN) foam produced by supercritical extraction of a phase-separated 10% PAN/dimethyl sulfoxide solution. This sample was made by R. Lagasse at Sandia National Laboratories. The plot is a compilation of data from static light scattering, Bonse–Hart X-ray, pin-hole X-ray in two geometries and X-ray diffraction (XRD) up to 40°. The Bonse–Hart and pin-hole data are in absolute intensity while the light-scattering and XRD data are scaled to match the absolute data. Extensive overlap of these data sets allows for accurate scaling. Light scattering is from the foam imbued with an index-matching solvent. Electron micrographs of the sample reveal a distorted rod structure in the 1 to 0.01 μm size range that corresponds to the first three decades of q in the plot. This has been previously referred to as a strut morphology (Aubert, 1988, 1991; Beaucage, Schaefer, Aubert, Lagasse, 1996) and has been related to spinodal decomposition in this system. An aspect ratio of 70 is common in micrographs. The scattering data in this size regime display power-law scaling with a power-law exponent of −1.61. R_s corresponds to a nano-structure within the struts that may be related to crystallinity. The marked difference between R_s and R_{sub} is seen in the data at $q = 10^{-2}$ Å^{-1}. R_{sub} corresponds well with the thickness of the struts in the strut morphology; R_g corresponds to the strut length.

The data are fitted to (9), 'Free Unified Fit', in Fig. 10. From this fit, the two size limits to the apparent-mass-fractal power-law regime are determined, $R_g = 0.82$ μm and $R_{sub} = 120$ Å. The larger R_g corresponds to the overall radius of gyration for the struts. This aspect ratio agrees with micrographs. The smaller, cutoff R_g, R_{sub}, is related to the radius of the struts. A third size scale is observed at higher q, $R_s = 66$ Å from (9), that is related to the base structure of the struts. Beyond this size, a power-law regime of slope −3.39 is observed. At still higher q, this surface-fractal regime decays into a power-law −4 or Porod regime (not fitted) before the onset of diffraction at highest q. The scattering for these smallest subunits of the structure is characteristic of fractally rough solid objects.

The data in Fig. 10 are also fitted using (9) and (8) to constrained the power-law prefactor, 'Unified Fit Under Polymeric Constraint'. In this fit, the high-q structural level was fixed to the values of the free fit and a least-squares optimization was used for the low-q data. For the constrainted fit, $P = 1.83$. The constrained fit does not match the data in the third and fourth decades of q. This is a typical case in which the material is an apparent mass-fractal (low-dimensional objects) and is therefore

not expected to be described by equations derived for deviations from polymeric structures. Equation (14) is expected to describe the power-law prefactor in this case.

Using (17), the surface area per gram for the microporous PAN sample of Fig. 10 is obtained. This sample has a density of 0.1 g cm^{-3} and bulk PAN has a density of 1.175 g cm^{-3}, thus $\varphi_p = 0.085$. From the unified fit, we have $G = 3.64 \times 10^6$ cm^{-1}, $B = 2.1$ cm^{-1} $Å^{-d_f}$, $d_f = 1.6$, $R_{sub} = 120$ Å and for a rod structure $R_{small\,dim} = 2/3^{1/2} R_{sub}$ (Beaucage, 1995; Beaucage & Schaefer, 1994). From a numerical integration over the free unified fit of Fig. 10, extrapolating the low-q region using a constant intensity of G and the high-q region using power-law -4 above $q = 0.39$ $Å^{-1}$, the invariant is obtained, $Q = 0.00809$ cm^{-1} $Å^3$. Using these values, $A \times (S/\text{mass}) = 393$ m^2 g^{-1}. For scattering from randomly distributed rods, $A = 4\pi^2/3^{3/2}$ and the surface area per gram is 51.7 m^2 g^{-1}. The nitrogen BET surface area for this sample is about 300 m^2 g^{-1}. This means that most of the surface area for the sample is derived from the 66 Å fractally rough structure seen in the fourth and fifth decades of q in Fig. 10.

As previously discussed, the surface area for a surface fractal (Hurd, Schaefer, Smith, Ross, Le Mehaute & Spooner, 1989; Bale, Schmidt, 1984; Wong & Bray, 1988) at a size of measurement r is given by $S(r) = Sr^{2-d_s}$ where $d_s = 2.61$ from Fig. 10. B for the high-q power-law regime is 0.000243 cm^{-1} $Å^{6-d_s}$. $F(d_s) = 1.82$, Q for the high-q structure $= 0.00468$ [using the last two terms of (9)], $S = 1390$ $Å^{2-d_s}$ m^2 g^{-1} and $S(r) = 1390 r^{-0.61}$. As noted above, for nitrogen absorption, Hurd (Hurd, Schaefer, Smith, Ross, Le Mehaute & Spooner, 1989) has used 4 Å for r yielding $(S/\text{mass})_{4\,Å} = 597$ m^2 g^{-1}. This value deviates from the specific surface area measured with nitrogen absorption because the actual cutoff to surface-fractal scaling occurs at a size larger than 4 Å.

Rather than using Hurd's nitrogen value of 4 Å for r, the transition size for surface fractal to Porod scattering should be used. The value of q at this transition can be determined by comparing a line of slope -4 to the data of Fig. 10 at high q. A rough estimate of $q = 0.39$ $Å^{-1}$ can be obtained in this manner. The r value for the transition from power-law -3.39 to -4 is $r = 2\pi/0.39$ $Å^{-1} = 16$ Å. Using $r = 16$ Å, $(S/\text{mass})_{16\,Å} = 256$ m^2 g^{-1}. This agrees well with the surface area measured by nitrogen absorption, about 300 m^2 g^{-1}. To reiterate, r in the determination of surface area from a surface fractal should correspond with either the transition size from surface fractal to Porod scattering, or to the size of the probe molecule in a gas-absorption measurement, depending on which is larger.

8. Conclusions

By the application of fractal ideas native to the disordered materials community to polymeric systems, deviations from ideal polymeric scaling can be described in a simple equation suitable for curve fitting. This functional form is developed through comparison of asymptotic forms for scattering from polymeric systems with a unified Guinier/power-law function. This approach can be extended to different regimes of power-law scattering through an extension of the structural level idea. For example, the transition from random walk to rod-like scattering at the persistence length of a polymer coil can be described using this approach.

This polymeric function can be, in turn, applied to mass-fractal disordered materials such as silica aerogels that display a wide variety of mass-fractal scaling. This leads to a better understanding of these disordered materials in terms of parameters common to the polymer field. Specifically, the degree of polymerization, the persistence length and the concept of a mer unit can all be used in describing these materials. This is used to estimate the surface area for these mass-fractal morphologies.

For polymer blends, this approach can account for deviations from ideal mass scaling. This allows an entire data set to be fitted in the RPA approach, rather than the conventional use of low-q fits that ignore the mass fractal scaling regime.

The approach presented here has been successful in describing a wide range of mass-fractal morphologies including fumed silica, low-density silica aerogels, colloidal silica gels and aerogels, polymeric microporous foams and gels as well as conventional polymeric systems (Beaucage, 1995; Beaucage & Schaefer, 1994; Beaucage, Ulibarri, Black & Schaefer, 1995; Ulibarri, Beaucage, Schaefer, Olivier & Assink, 1992; Hua, Anderson, Hareid, Smith & Beaucage, 1994; Schaefer, Pekala & Beaucage, 1995). Deviations from the polymeric mass-fractal approach are seen in systems with asymmetric structural units such as in randomly oriented lamellar and rod systems. For these cases, an approach to the determination of surface area and power-law exponents was discussed. Apparent mass fractals can be distinguished from polymeric mass fractals by comparison of the power-law prefactor in the scattering pattern.

Some of this work was performed at Sandia National Laboratories supported by the US Department of Energy (DOE) by Sandia National Laboratories under Contract #DE-AC04-94AL85000. Polymer foams were supplied by J. Aubert and R. Lagasse; isotropic PS blends were supplied by M. Satkowski and S. Smith and some aerogel data were supplied by Dale W. Schaefer and C. Ashley. Detailed papers on these systems are in preparation. Neutron scattering data were obtained at Los Alamos National Laboratory, Oak Ridge National Laboratory and the National Institute of Standards and Technology. Ultra-low-q SAXS measurements were made at NIST's X23A3 beamline at Brookhaven National Laboratories

National Synchrotron Light Source, the use of which was courtesy of G. Long and D. Fischer (Long, Jemain, Weertman, Black, Burdette & Spal, 1991). Pin-hole SAXS data are from Oak Ridge National Laboratories, courtesy of J. S. Lin.

References

Aubert, J. H. (1988). *Macromolecules*, **21**, 3468–3474.

Aubert, J. H. (1991). *Polymer Preprints*, **32**, 420–476.

Bale, H. D. & Schmidt, P. W. (1984). *Phys. Rev. Lett.* **53**, 596–599.

Beaucage, G. (1995). *J. Appl. Cryst.* **28**, 717–728.

Beaucage, G. & Schaefer, D. W. (1994). *J. Non-Cryst. Solids*, **172–174**, 797–805.

Beaucage, G., Schaefer, D. W., Aubert, J. H. & Lagasse, R. (1996). In preparation.

Beaucage, G. & Stein, R. S. (1993*a*). *Macromolecules*, **26**, 1609–1616.

Beaucage, G. & Stein, R. S. (1993*b*). *Macromolecules*, **26**, 1617–1626.

Beaucage, G., Stein, R. S. & Koningsveld, R. (1993). *Macromolecules*, **26**, 1603–1608.

Beaucage, G., Ulibarri, T. A., Black, E. & Schaefer, D. W. (1995). *Organic Hybrid Materials*, edited by J. E. Mark, C. Y.-C. Lee & P. A. Bianconi, p. 97. *ACS Symposium Series* No. 585. Washington, DC: American Chemical Society.

Benoit, H. (1957). *Compt. Rend.* **245**, 2244–2247.

Bondi, A. (1964). *J. Phys. Chem.* **68**, 441–451.

Brinker, C. J. & Scherer, G. W. (1990). *Sol-Gel Science, the Physics and Chemistry of Sol-Gel Processing*. New York: Academic Press.

Debye, P. (1945). Tech. Rep. 637 to Rubber Reserve Co., reprinted in Debye, P. (1954). *The Collected Papers of Peter J. W. Debye*. New York: Interscience.

Debye, P. (1947). *J. Phys. Colloid. Chem.* **51**, 18–32.

Debye, P., Henderson, H. R. & Brumberger, H. (1957). *J. Appl. Phys.* **28**, 679–683.

Feigin, L. A. & Svergun, D. I. (1987). *Structural Analysis by Small Angle X-ray and Neutron Scattering*, p. 84. New York: Plenum Press.

Fischer, M. E. & Burford, R. J. (1967). *Phys. Rev.* **156**, 583–622.

Gennes, P. de (1979). *Scaling Concepts in Polymer Physics*. Ithaca, NY: Cornell University Press.

Guinier, A. & Fournet, G. (1955). *Small-Angle Scattering of X-rays* John Wiley and Sons, NY pp. 27–28.

Heimenz, P. C. (1984). *Polymer Chemistry*, p. 54. New York: Marcel Dekker.

Hua, D. W., Anderson, J., Hareid, S., Smith, D. M. & Beaucage, G. (1994). *Better Ceramics through Chemistry 6*, edited by A. K. Cheetham, C. J. Brinker, M. L. Mecartney & C. Sanchez, p. 985. Materials Research Society Proceedings Vol. 346. Pittsburgh, PA: Materials Research Society.

Hurd, A. J. (1990). *Optical Fiber Materials and Processing*, edited by J. W. Fleming, G. H. Sigel, S. Takahashi & P. W. France, p. 3. Materials Research Society Proceedings Vol. 172. Pittsburgh, PA: Materials Research Society.

Hurd, A. J., Schaefer, D. W., Smith, D. M., Ross, S. B., Le Mehaute, A. & Spooner, S. (1989) *Phys. Rev. B*, **39**, 9742–9745.

Korberstein, J. T., Morra, B. & Stein, R. S. (1980). *J. Appl. Cryst.* **13**, 34–45.

Kurata, M. & Tsunashima, Y. (1989). in *Polymer Handbook*, 3rd ed., p. VII/1–3. New York: Wiley.

LeMay, J. D., Hopper, R. W., Hrubesh, L. W. & Pekala, R. W. (1990). *Mater. Res. Soc. Bull.* **15**, 19–45.

Lin, M. Y., Klein, R., Lindsay, H. M., Weitz, D. A., Ball, R. C. & Meakin, P. (1990) *J. Col. Interface Sci.* **137**, 263–280.

Long, G. G., Jemain, J. R., Weertman, J. R., Black, D. R., Burdette, H. E. & Spal, R. (1991). *J. Appl. Cryst.* **24**, 30–39.

Mountain, R. D. & Mulholland, G. W. (1988). *Langmuir*, **4**, 1321–1326.

Mountain, R. D., Mulholland, G. W. & Baum, H. (1986). *J. Colloid Interface Sci.* **114**, 67–81.

Peterlin, A. (1953). *Makromol. Chem.* **9**, 244–268.

Schaefer, D. W. & Hurd, A. J. (1990). *Aerosol Sci. Technol.* **12**, 876–890.

Schaefer, D. W., Martin, J. E. & Keefer, K. D. (1985), pp. 31, in *Physics of Finely Divided Matter*, eds. N. Bocarra and M. Daoud, Springer-Verlag, Berlin.

Schaefer, D. W., Olivier, B. J., Ashley, C. S., Richter, D., Farago, B., Frick, B., Hrubesh, L., van Bommel, M. J., Long, G. & Krueger, S. (1992). *J. Non-Cryst. Solids*, **145**, 105–112.

Schaefer, D. W., Pekala, R. & Beaucage, G. (1995). *Macromolecules*. In the press.

Schmidt, P. W. (1992). *J. Appl. Cryst.* **15**, 567–569.

Schmitz, K. S. (1990). *An Introduction to Dynamic Light Scattering by Macromolecules*, pp. 57–65. New York: Academic Press.

Tsvetkov, V. N. & Andreeva, L. N. (1989). *Polymer Handbook*, 3rd ed., p. VII/577. New York: Wiley.

Ulibarri, T. A., Beaucage, G., Schaefer, D. W., Olivier, B. J. & Assink, R. A. (1992). *Submicron Multiphase Materials*, edited by R. H. Baney, L. R. Gilliom, S. Hirano, & H. K. Schmidt. Materials Research Society Symposium Proceedings Vol. 274, Materials Research Society, Pittsburg, PA.

Wiltzius, P., Bates, F. S., Dierker, S. B. & Wignall, G. D. (1987). *Phys. Rev. A*, **36**, 2991–2994.

Wong, P. & Bray, A. J. (1988). *J. Appl. Cryst.* **21**, 786–794.